Lower Bounds on Acceleration Estimation Accuracy

K.-P. Dunn

5 October 1987

Lincoln Laboratory

MASSACHUSETTS INSTITUTE OF TECHNOLOGY

LEXINGTON, MASSACHUSETTS

ADA 188383

This technical report has been reviewed and is approved for publication.

FOR THE COMMANDER

Arthur H. Wendel, Captain, USAF
Acting Chief, ESD Lincoln Laboratory Project Office

MASSACHUSETTS INSTITUTE OF TECHNOLOGY
LINCOLN LABORATORY

LOWER BOUNDS ON ACCELERATION ESTIMATION ACCURACY

K.-P. DUNN
Group 32

TECHNICAL REPORT 790

5 OCTOBER 1987

LEXINGTON   MASSACHUSETTS

ABSTRACT

Estimation lower bounds on the accuracy of radar measurement of the acceleration of a moving target are derived. These bounds are expressed in terms of the sensor parameters, such as: range (or Doppler) and angle accuracies, track time, data rate (PRF), and an *a priori* estimate of the direction of the target acceleration. Simple scaling laws that allow the reader to trade-off these parameters utilizing curves presented in this report are also given.

TABLE OF CONTENTS

LIST OF ILLUSTRATIONS

LIST OF ILLUSTRATIONS (Continued)

LOWER BOUNDS ON ACCELERATION ESTIMATION ACCURACY

I. INTRODUCTION

To determine tracking sensor measurement accuracy requirements for determining, or detecting a change in target acceleration often requires numerous computer simulations for various sensor-target geometries, sensor measurement accuracies, data rate (PRF) and total track time. This exercise is generally very time-consuming and very inefficient in studying sensor parameter trade-offs for a sensor system design. Furthermore, numerical results obtained by this approach are extremely sensitive to the particular tracking algorithm used in the simulation study.

In this report, an analytical formula is derived for calculating lower bounds on acceleration measurement accuracy with given sensor-target geometry and sensor parameters such as: range (or Doppler) and angle measurement accuracies, data rate (PRF) and total track time. Given a system requirement on the acceleration accuracy, a set of sensor parameters can be determined by this formula such that the computed lower bound on acceleration measurement meets the requirement. These sensor parameters are often slightly optimistic. To show that these theoretical lower bounds can be achieved with the selected sensor parameters, an acceleration estimation algorithm will have to be developed and simulated with these parameters. However, previous work [1] has shown that, for small measurement errors, the lower bounds can be achieved. With no specific system requirements on the acceleration measurement given in this report, families of lower bounds will be generated for various values of sensor parameters. Some interesting formulas and scaling laws will also be given for quick calculations needed in sensor trade-off studies.

This report is organized as follows: In the next section, the analytical formulas for calculating lower bounds on acceleration estimation accuracy are derived. Numerical examples are given in Section III. Interpretation of these results will also be presented. Finally, a brief summary will be given in Section IV.

1

II. ACCELERATION ESTIMATION LOWER BOUNDS

In this section, we will determine lower bounds on the acceleration measurement accuracy for a radar with given range (or Doppler) and angle accuracy tracking an accelerating target for the case in which there is a given *a priori* estimate of the direction of the target acceleration. To derive these bounds, we will first assume that the direction of the target acceleration is given so that the acceleration estimation accuracies along the line-of-sight vector and the direction normal to it in the trajectory plane can be determined as a function of radar measurement parameters. These estimation accuracies are then used to derive acceleration measurement accuracy lower bounds for cases when the direction of the target acceleration is not known precisely.

Consider an object moving with a velocity V with a look angle ß with respect to an observer at a range R as depicted in Figure 1. An acceleration of magnitude, a, is applied to the object at the time of observation along a direction making an angle α with respect to the line-of-sight vector **R** as shown in Figure 1. For simplicity, we assume **V**, **a** and **R** are coplanar, although the results are not sensitive to this assumption.
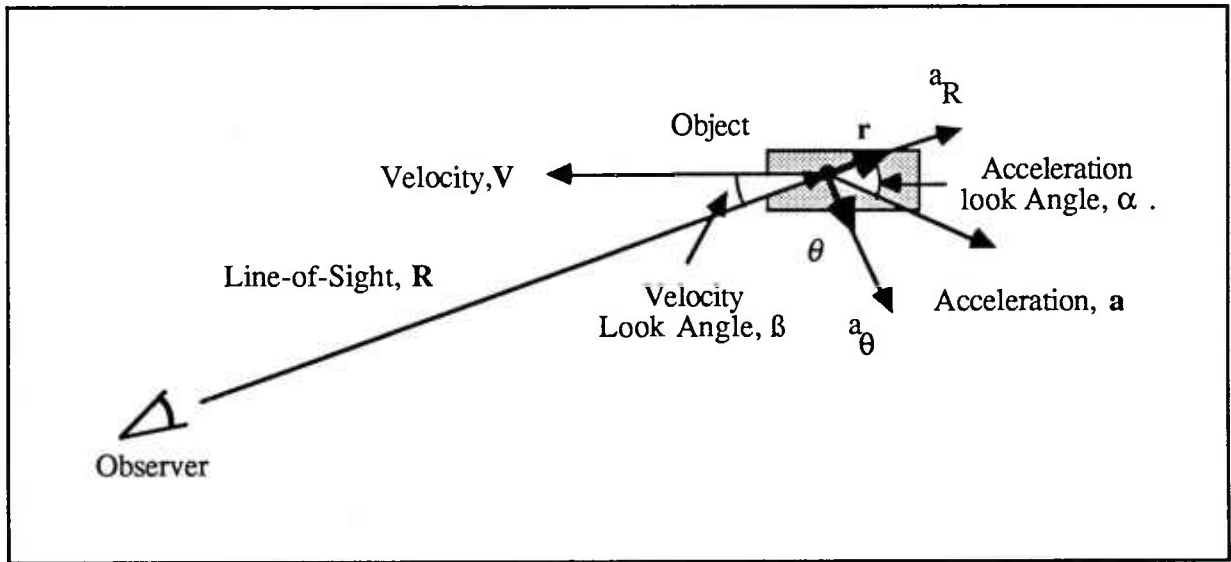
Figure 1.   Object and observer geometry.

Using a polar coordinate system, the acceleration vector can be represented as:

$$\mathbf{a} = (\ddot{R} - R\dot{\theta}^2)\,\mathbf{r} + (R\ddot{\theta} + 2\dot{R}\dot{\theta})\,\theta \qquad (1)$$

where $\mathbf{r}$ is the unit vector along the line-of-sight and θ the unit vector normal to $\mathbf{r}$ in the ($\mathbf{R,a}$)-plane. $\dot{R}, \dot{\theta}, \ddot{R}$ and $\ddot{\theta}$ are magnitudes of range and angle velocities and accelerations, respectively.

Let a_R and a_θ be the components of $\mathbf{a}$ along $\mathbf{r}$ and θ as follows:

$$a_R = \ddot{R} - R\dot{\theta}^2$$

$$\qquad (2)$$

$$a_\theta = R\ddot{\theta} + 2\dot{R}\dot{\theta}$$

Taking the first order perturbation of (2) around (a_R, a_θ), we have

$$\Delta a_R = \Delta\ddot{R} - \dot{\theta}^2\Delta R - 2R\dot{\theta}\Delta\dot{\theta}$$

$$\qquad (3)$$

$$\Delta a_\theta = \ddot{\theta}\,\Delta R + R\Delta\ddot{\theta} + 2\dot{\theta}\Delta\dot{R} + 2\dot{R}\Delta\dot{\theta}$$

where $R\dot{\theta} = V\sin\beta$. For the case considered in this report, we have

$$R \gg V \quad \text{that is } \dot{\theta} \ll 1/\text{sec.}$$

Therefore, the acceleration estimate along the $\mathbf{r}$ and θ directions can be approximated by the following:

$$\sigma^2_{a_R} = \sigma^2_{\ddot{R}} + (2V\sin\beta)^2\sigma^2_{\dot{\theta}}$$

$$\qquad (4)$$

$$\sigma^2_{a_\theta} = R^2\sigma^2_{\ddot{\theta}} + (2V\sin\beta/R)^2\sigma^2_{\dot{R}} + (2V\cos\beta)^2\sigma^2_{\dot{\theta}}$$

The relation of (4) to the sensor single hit measurement accuracy in range, angle and Doppler is derived in the Appendix.

If the angle α is given, as shown in Figure 2, the overall acceleration accuracy can be computed by the following formula:

$$\sigma_a^2 = \left[\left[\frac{\sigma_{a_R}^2}{\cos^2\alpha} \right]^{-1} + \left[\frac{\sigma_{a_\theta}^2}{\sin^2\alpha} \right]^{-1} \right]^{-1} \tag{5}$$

$$1\sigma \quad \text{ERROR ELLIPSE:}$$

$$1 = \frac{\sigma_a^2 \cos^2\alpha}{\sigma_{a_R}^2} + \frac{\sigma_a^2 \sin^2\alpha}{\sigma_{a_\theta}^2}$$

Figure 2. Acceleration estimation accuracy given acceleration direction.

In this case, σ_a is generally close to the smaller of σ_{a_R} or σ_{a_θ}, if these components are very different in magnitude. This formula was used in an earlier radar study to determine the radar
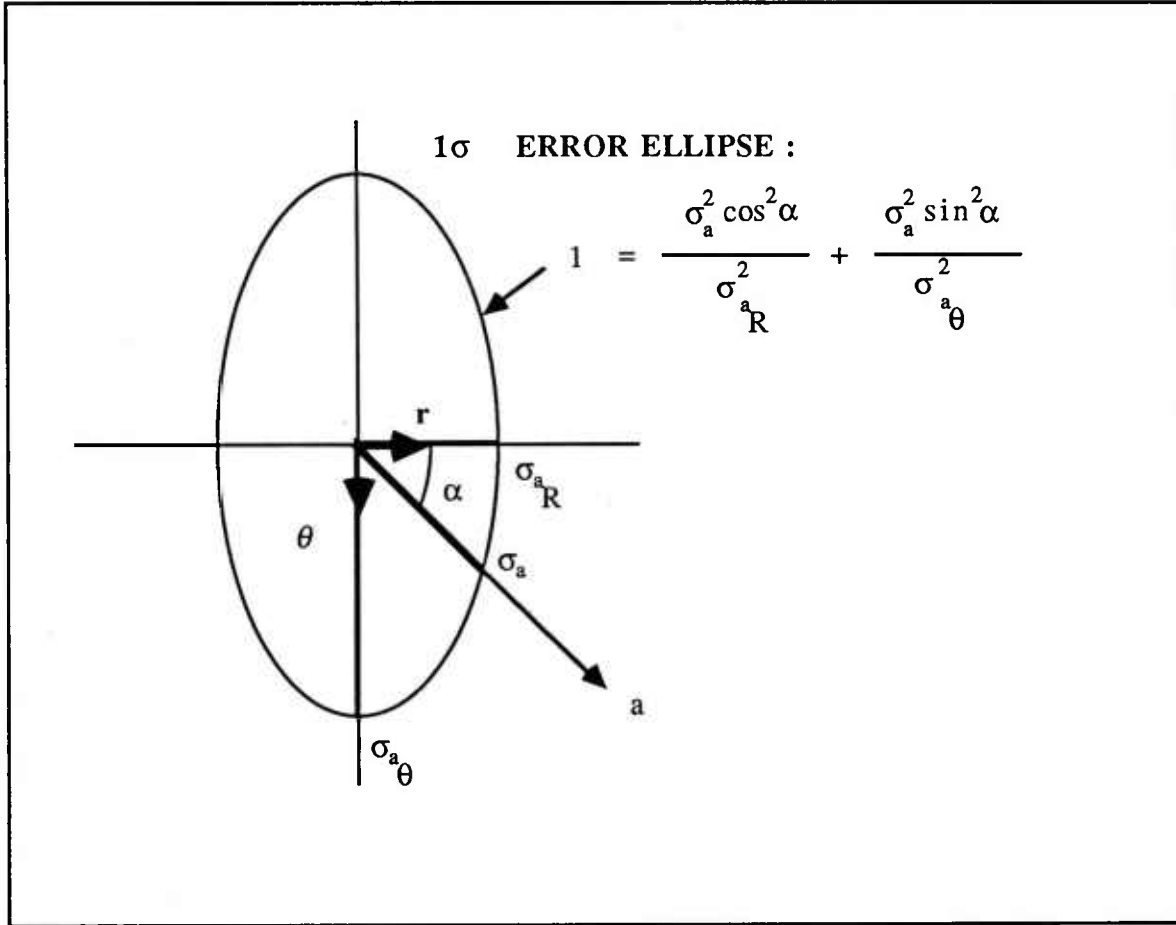
requirements. On the other hand, if the angle α is completely unknown, then the total acceleration error is the root-sum-square of the errors along $\mathbf{r}$ and θ projected onto $\mathbf{a}$, that is

$$\sigma_a^2 = \sigma_{a_R}^2 \cos^2\alpha + \sigma_{a_\theta}^2 \sin^2\alpha \qquad (6)$$

In this case, σ_a is generally close to the larger of σ_{a_R} or σ_{a_θ}. Figure 3 shows a plot of $\sigma_a = 1g$ in the σ_{a_R} - σ_{a_θ} plane for both Eq.(5) and Eq.(6). In most cases, the angle α is obtained by tracking the target before and after the acceleration change or by other *a priori* information. The accuracy of this angle estimate can be varied dramatically depending upon the assumptions made. In the following paragraph, we will derive a formula which takes this uncertainty into account parametrically.

As illustrated in Figure 1, two components of the acceleration of an object can be measured by a sensor, a_R and a_θ. The knowledge of α can be modelled as a measurement obtained by the sensor with an accuracy σ_α. The Cramer Rao lower bound on any unbiased estimate of the acceleration magnitude, a, can be derived with the following measurement equations [2]:

$$a_R = a \cos\alpha + n_R$$

$$a_\theta = a \sin\alpha + n_\theta \qquad (7)$$

$$\alpha' = \alpha + n_\alpha$$

where n_R, n_θ, and n_α are independent Gaussian random variables with zero means and standard deviations σ_{a_R}, σ_{a_θ} and σ_α. Following the steps in [2] and using Eq.(7), we have

$$\sigma_a^2 = \frac{\sigma_{a_R}^2 \sigma_{a_\theta}^2 + a^2 \sigma_\alpha^2 (\sigma_{a_\theta}^2 \sin^2\alpha + \sigma_{a_R}^2 \cos^2\alpha)}{a^2 \sigma_\alpha^2 + (\sigma_{a_\theta}^2 \cos^2\alpha + \sigma_{a_R}^2 \sin^2\alpha)} \qquad (8)$$
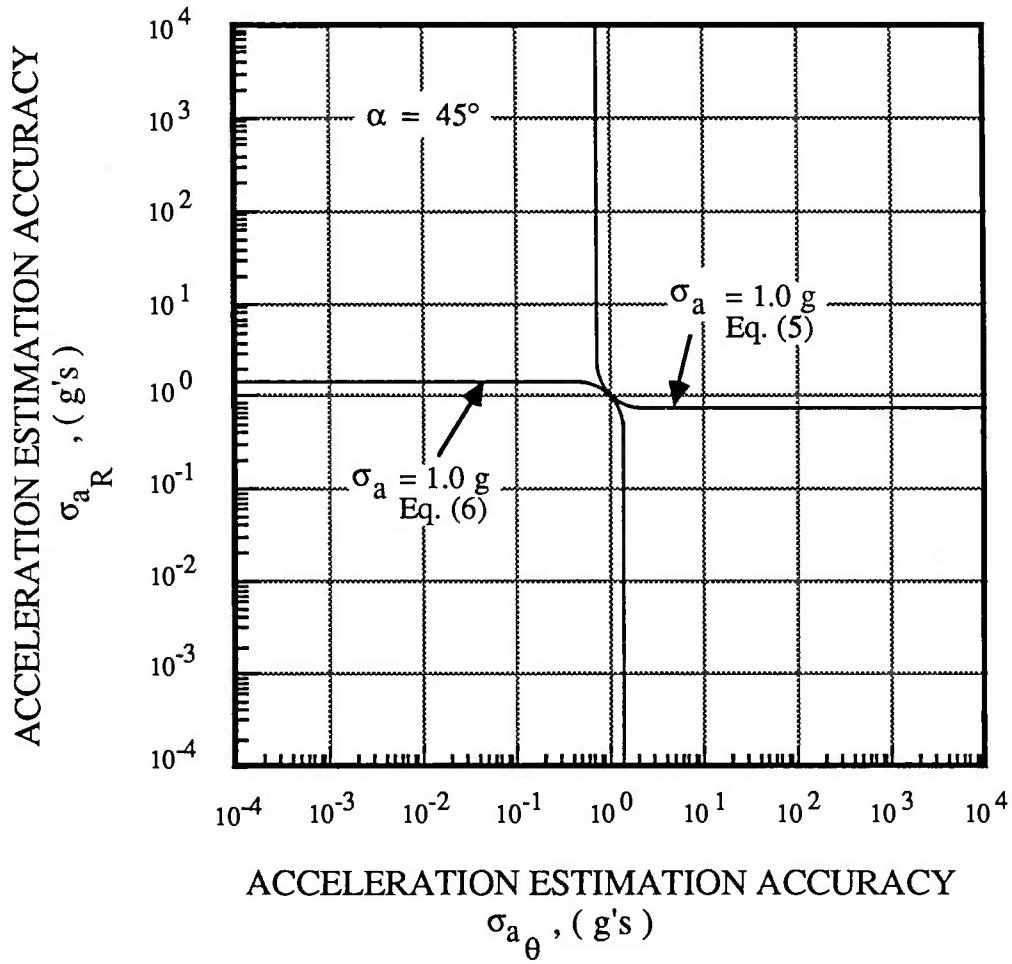
Figure 3. Overall acceleration estimation accuracy as a function of σ_{a_R} and σ_{a_θ} for both Eq.(5) and Eq.(6).

Combining Eqs. (8), (4) and (A.1) through (A.4) of the Appendix gives the overall acceleration estimation accuracy for a given *a priori* estimate of α with accuracy σ_α. Notice that Eqs. (5) and (6) can be derived from Eq. (8) for $\sigma_\alpha = 0°$ and $\infty°$, respectively.

In the following section, numerical examples will be given without a specific system design requirement. Most of the results were generated by an EXCEL spreadsheet program on a Macintosh computer.

III. NUMERICAL EXAMPLES AND INTERPRETATION OF RESULTS

The acceleration estimation accuracies along the **r** and θ directions of Eq. (4) are shown in Figure 4 and Figure 5, respectively, for a wide range of values of radar range and angle measurement accuracies[1],[2]. An arbitrary sensor-target geometry indicated in both figures is chosen throughout this report. Every curve shown in both figures has the same general shape depicted in Figure 6. It consists of two important asymptotes; the horizontal asymptote represents the errors dominated by the range measurement accuracy and the sloped asymptote represents errors dominated by the angular measurement accuracy. The acceleration estimation accuracies at these limits are linearly proportional to the range or the angle measurement accuracy as follows:

$$\lim_{\varepsilon_\theta \to 0} \sigma_{a_R} = \sigma_{\ddot{R}} = \sqrt{\frac{720}{N(N^2-1)(N^2-4)}} \frac{\varepsilon_R}{T^2} \qquad (9)$$

$$\lim_{\varepsilon_R \to 0} \sigma_{a_R} = 2V\sin\beta \, \sigma_{\dot{\theta}} = 2V\sin\beta \sqrt{\frac{12}{N(N^2-1)}} \frac{\varepsilon_\theta}{T} \qquad (10)$$

$$\lim_{\varepsilon_\theta \to 0} \sigma_{a_\theta} = (2V\sin\beta/R)\sigma_{\dot{R}} = (2V\sin\beta/R)\sqrt{\frac{12}{N(N^2-1)}} \frac{\varepsilon_R}{T} \qquad (11)$$

$$\lim_{\varepsilon_R \to 0} \sigma_{a_\theta} = R\sigma_{\ddot{\theta}} = R\sqrt{\frac{720}{N(N^2-1)(N^2-4)}} \frac{\varepsilon_\theta}{T^2} \qquad (12)$$

---

[1] The range of radar measurement accuracies appearing in all figures of this report is not intended to represent realistic sensor measurement capabilities; but is meant to present, mathematically, the entire picture of acceleration measurement accuracy as a function of radar measurement accuracies.

[2] Notice that σ_{a_R} is more sensitive to σ_R than is σ_{a_θ} for these parameters.
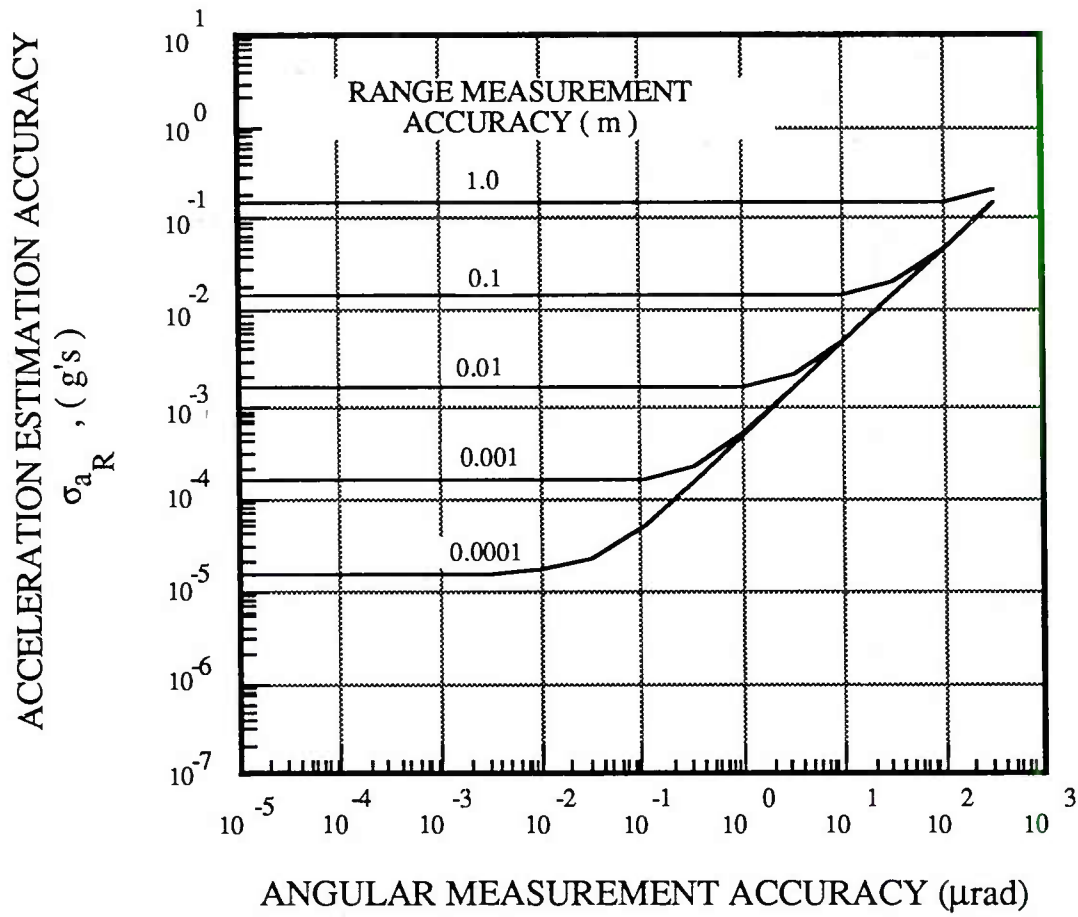
Figure 4. Acceleration estimation accuracy along **r** as a function of radar range and angle measurement accuracies.

9
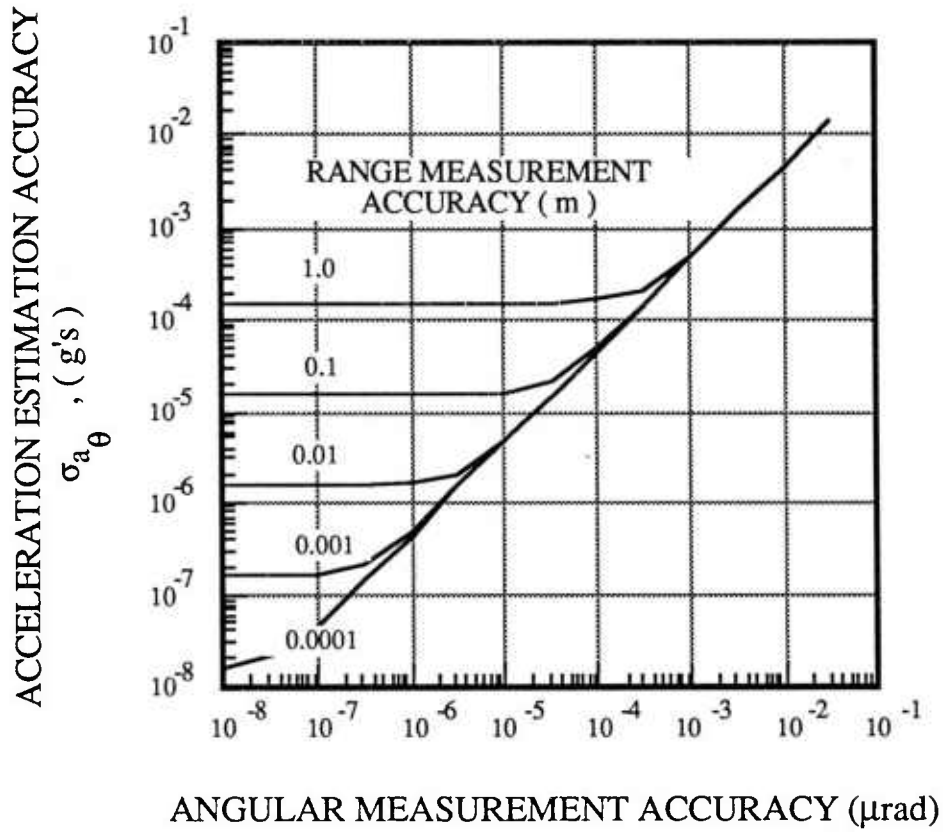
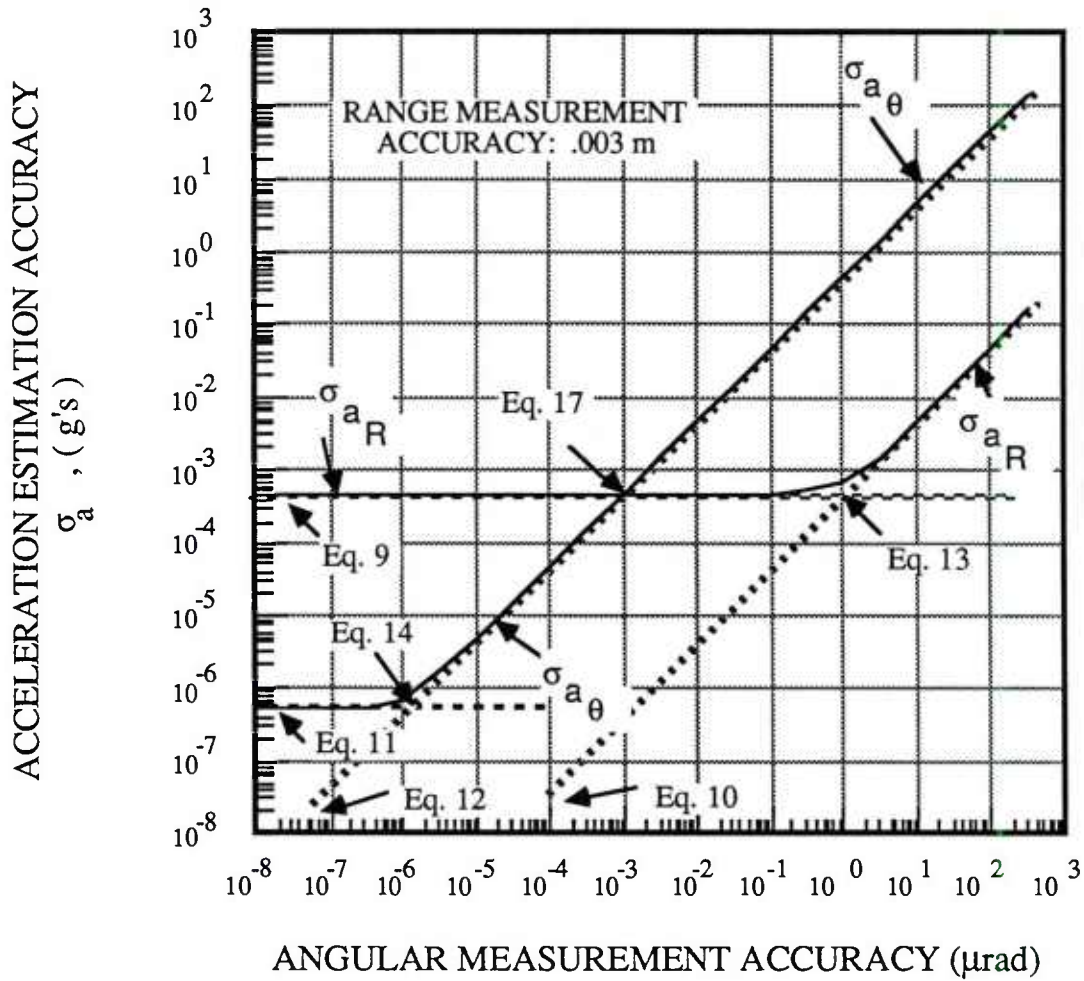Figure 5. Acceleration estimation accuracy along θ as a function of radar range and angle measurement accuracies.

10

Figure 6. Acceleration estimation accuracies in both r and θ directions. Equations that compute the limiting values of these curves, intersection points of their asymptotes, and intersection point of these two curves are indicated.

11

The intersection point of these two asymptotes is also interesting and gives a rough estimate of the location at which the range and angle measurements are equally important. It can be computed by the following formulas:

$$\text{For} \quad \sigma_{a_R}: \quad \varepsilon_\theta = \sqrt{\frac{60}{(N^2-4)}} \; \frac{\varepsilon_R}{2V\sin\beta\, T} \qquad (13)$$

$$\text{For} \quad \sigma_{a_\theta}: \quad \varepsilon_R = \sqrt{\frac{60}{(N^2-4)}} \; \frac{R^2\varepsilon_\theta}{2V\sin\beta\, T} \qquad (14)$$

Furthermore, the following inequalities hold.

$$\text{If} \quad \sqrt{\frac{60}{(N^2-4)}} \; \frac{R}{2V\sin\beta\, T} > 1, \text{ then} \qquad (15)$$

$$\text{For a given } \varepsilon_R, \qquad \lim_{\varepsilon_\theta \to 0} \sigma_{a_R} > \lim_{\varepsilon_\theta \to 0} \sigma_{a_\theta} \quad , \text{ and}$$

$$\text{For a given } \varepsilon_\theta, \qquad \lim_{\varepsilon_R \to 0} \sigma_{a_\theta} > \lim_{\varepsilon_R \to 0} \sigma_{a_R} \qquad (16)$$

If the inequality in (15) reverses direction, so do the inequalities in (16). This implies that these two curves will always intersect and will intersect at

$$\varepsilon_R = R\,\varepsilon_\theta \qquad (17)$$

for all given range measurement accuracies. When the range and cross-range position accuracies are equal, the range and cross-range acceleration accuracies will be equal.

We now combine σ_{a_R} and σ_{a_θ} to determine σ_a. Figure 7 shows the overall acceleration estimation accuracy, Eq. (8), as a function of σ_α. Notice that the following formulas are very good approximations to Eqs. (5) and (6):

$$\sigma_a(\sigma_\theta) \cong \begin{cases} \text{Max } \{\sigma_{a_R}(\sigma_\theta), \sigma_{a_\theta}(\sigma_\theta)\} & \text{for } \alpha \text{ unknown} \\ \\ \text{Min } \{\sigma_{a_R}(\sigma_\theta), \sigma_{a_\theta}(\sigma_\theta)\} & \text{for } \alpha \text{ given} \end{cases} \qquad (18)$$

to within factors of $\sin\alpha$ or $\cos\alpha$. Figure 8 shows a family of curves of σ_a with different values of range measurement accuracy, ε_R, for $\sigma_\alpha = 0°$. Consider the curve for range measurement accuracy $\varepsilon_R = 0.01$ m. For angular measurement accuracy ε_θ larger than 10 μrad, σ_a decreases as ε_θ decreases. The curve reaches a plateau between $\varepsilon_\theta = 1$ and 10^{-2} μrad. This portion of the curve corresponds to the case where $\sigma_{a_R} < \sigma_{a_\theta}$ and σ_{a_R} has reached its horizontal asymptote. As ε_θ decreases further, $\sigma_{a_R} > \sigma_{a_\theta}$ and σ_a decreases again. Finally, for $\varepsilon_\theta < 10^{-6}$ μrad, σ_{a_θ} has reached its horizontal asymptote and σ_a will not decrease further.

If we held σ_a constant, say 0.01g as shown by dotted line in Figure 8, and trade-off range and angle measurement accuracy, we obtain a contour shown in Figure 9. Similarly, contours for different values of σ_α can be obtained as was done in Figure 9. The asymptotes and knees of each contour can be approximated by equations indicated in Figure 6 and Eq.(8) for each given value of σ_a and σ_α. Figures 10, 11 12 and 13 show a family of contours for different values of σ_a for σ_α at 0°, 1°, 10° and infinity, respectively. Notice that there are two plateaus as indicated in Figures 11 and 12: "Plateau R" is the region where σ_a varies very slowly as the range measurement accuracy changes for a couple order of magnitudes, and "Plateau A" corresponds to a similar region for the angle measurements. These contours are plotted for σ_a between 0.3 to 0.001g. Contours with σ_a values outside this range will have the same shape as the contour of $\sigma_a = 0.3$g and 0.001g. This will be more apparent when σ_a is displayed by a 3-D graph. The same set of σ_α values are used to generate 3-D graphs as shown in Figures 14, 15, 16 and 17.

Figure 18 shows trade-off contours of range and angle measurement accuracy requirement for $\sigma_a = 0.03$g with the same set of σ_α. In region A, we have extremely accurate range measurement where $\sigma_{a_R} \ll \sigma_{a_\theta}$ and $\sigma_a \sim \sigma_{a_R}$. Eq.(10) should be used to determine the value of the angle measurement accuracy required for a given σ_a. σ_a is determined primarily by ε_θ. In region B, we have more accurate angle measurements than those in region A but we still have

$\sigma_{a_R} < \sigma_{a_\theta}$. $\sigma_a \sim \sigma_{a_R}$ and depends primarily on the range measurement accuracy. Eq.(9) should be used to determine the value of range measurement accuracy required for a given σ_a. A similar trade-off applies to regions C and D by interchanging R and θ everywhere in the discussion for regions A and B, respectively. In region E, $\sigma_{a_R} \sim \sigma_{a_\theta}$ and σ_a is not sensitive to the value of σ_α. The requirements on both range and cross-range position accuracies are equal.

We now look at how σ_a scales with track time and data rate. Rewriting Eqs. (9) - (12), in terms of the PRF (1/T) and the total track time (NT) we see that the acceleration accuracy varies as $T^{1/2}$, and $(NT)^{-3/2}$ or $(NT)^{-5/2}$ depending on the relative angle and range accuracy. Figure 19 shows a family of σ_a curves as a function of PRF for a total track time of 10 seconds with a fixed ε_R and different values of ε_θ. Notice that the spaces between curves are not uniform in some regions of ε_θ; this is due to the fact that in some regions, the range measurement dominates while in others the angle measurement dominates. Figure 20 shows a family of σ_a curves as a function of the total track time for a fixed PRF of 10 Hz. and fixed ε_R and different values of ε_θ. Notice that all curves eventually converge to the slope of -3/2 as the total track time increases. This is because the -3/2th power of the total track time converges to zero slower than the -5/2th power of NT. The transition points can be calculated from Eqs. (9) - (12). Similar curves like those shown in Figures 19 and 20 are given in Figures 21 and 22 for $\sigma_\alpha = \infty$. Notice that in Figure 22 the slopes of all curves are -5/2. This is because for $\sigma_\alpha = \infty$ only Eqs. (9) and (12) apply to these cases.

To obtain results for Doppler-only cases, one can scale the results for range-only cases by a factor of $[\, 60/(N^2 - 4)]^{1/2} / T$. This follows from Eq. (A-2). A family of curves where range and Doppler measurements give same range acceleration accuracy are given in Figure 23. If both range and Doppler are available, the performance is determined primarily by the more accurate one. That is, above the curves in Figure 23, the range measurements are more useful while below the curves, the Doppler measurements are more useful.

R = 3000 km   V = 7 km/sec.   a = 0.2 g

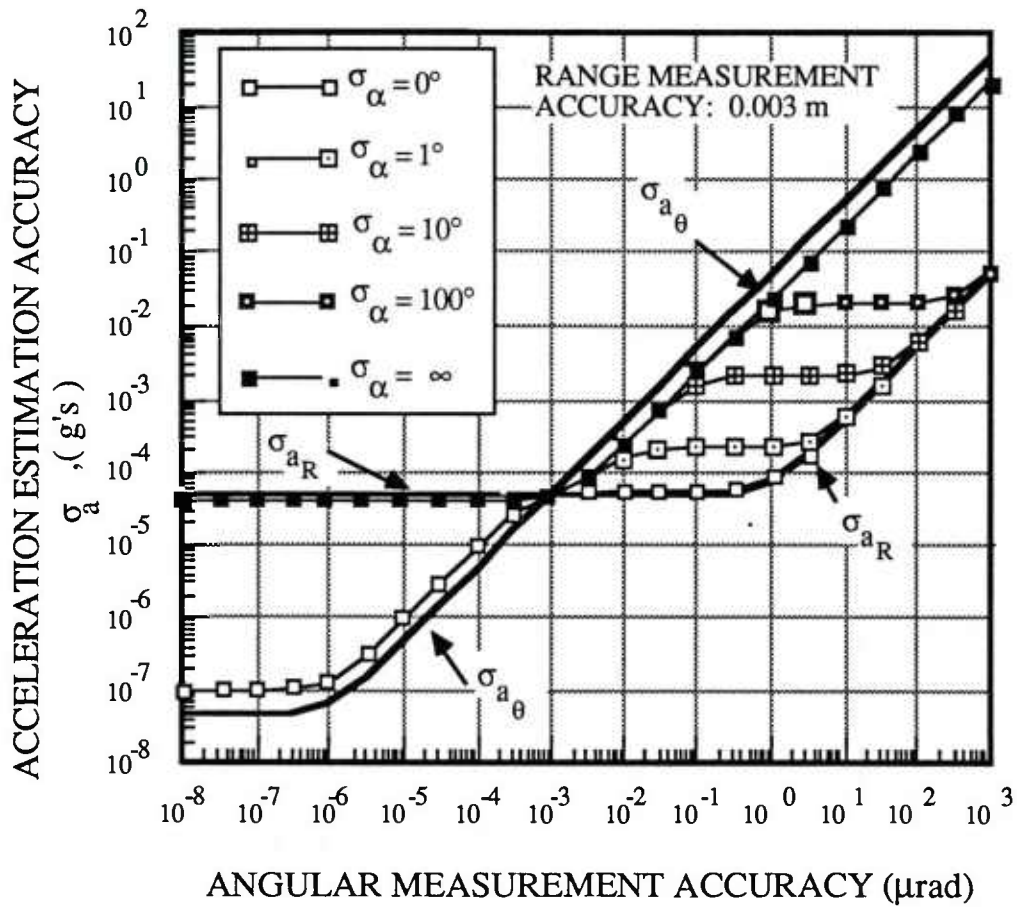α = 30°   ß = 60°   PRF = 10 Hz.   NT = 2 sec

Figure 7. Overall acceleration estimation accuracy as a function of angular measurement accuracy and *a priori* knowledge of acceleration direction, α.

R = 3000 km   V = 7 km/sec.   a = 0.2 g

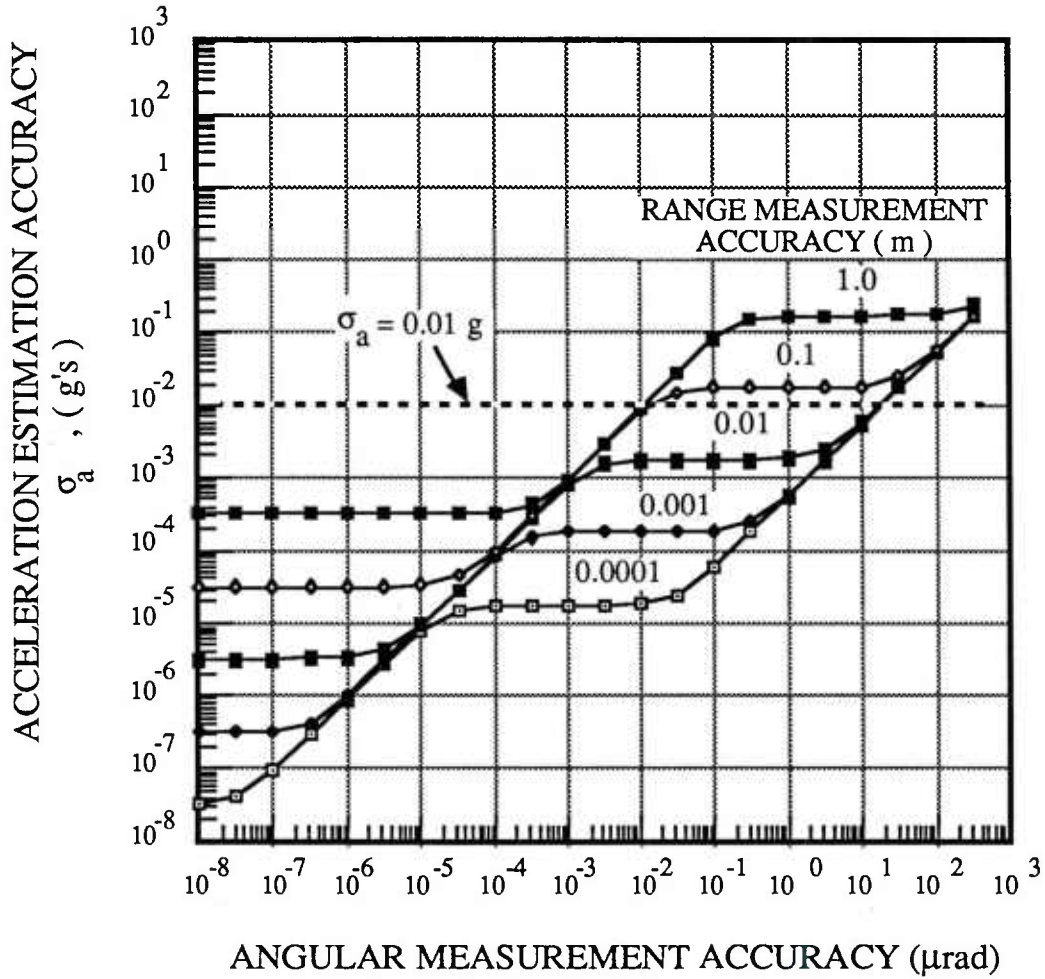α = 30°   ß = 60°   PRF = 10 Hz.   NT = 2 sec

Figure 8. Overall acceleration estimation accuracy as a function of angular measurement accuracy for various range measurement accuracies with $\sigma_\alpha = 0°$.

16

R = 3000 km   V = 7 km/sec.   a = 0.2 g

α = 30°   ß = 60°   PRF = 10 Hz.   NT = 2 sec

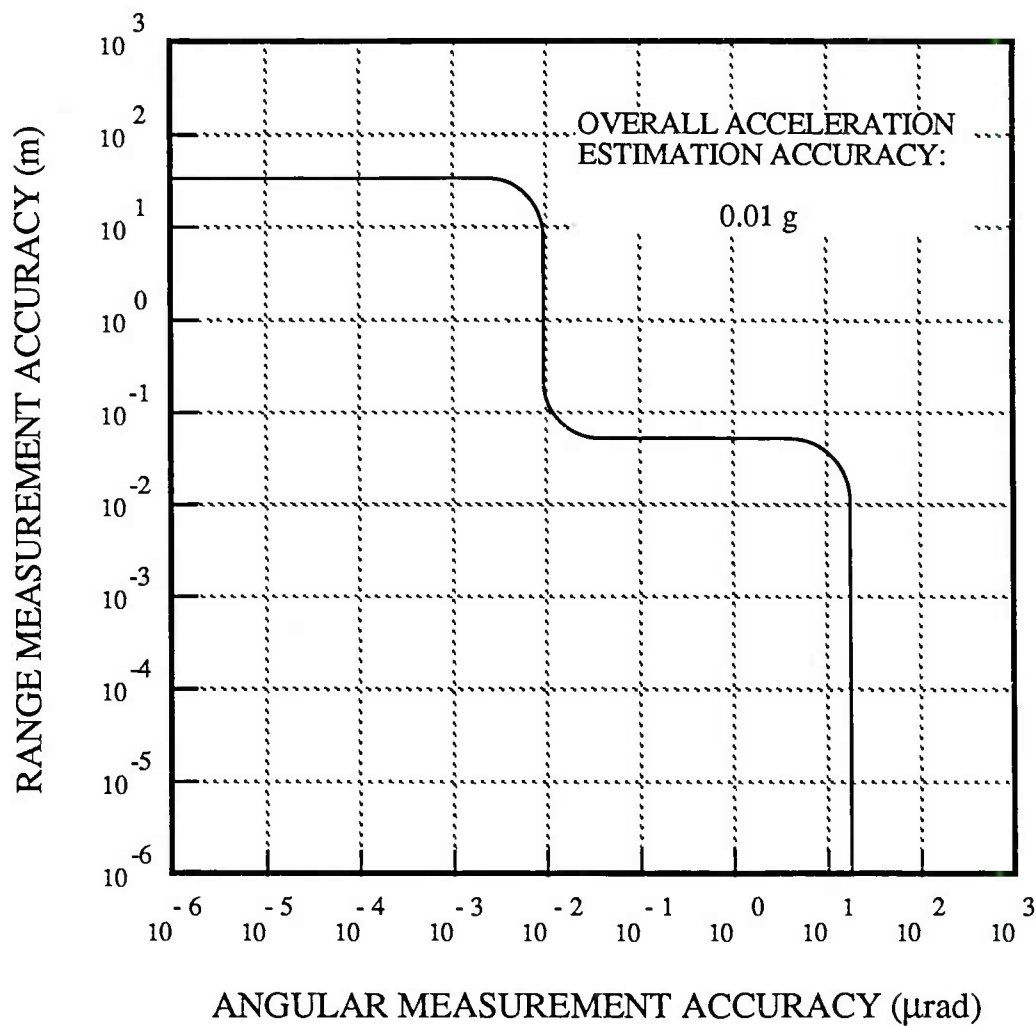OVERALL ACCELERATION ESTIMATION ACCURACY:

0.01 g

Figure 9. A contour of overall acceleration estimation accuracy at 0.01g is plotted as a function of radar angle and range measurement accuracies with $\sigma_\alpha = 0°$.
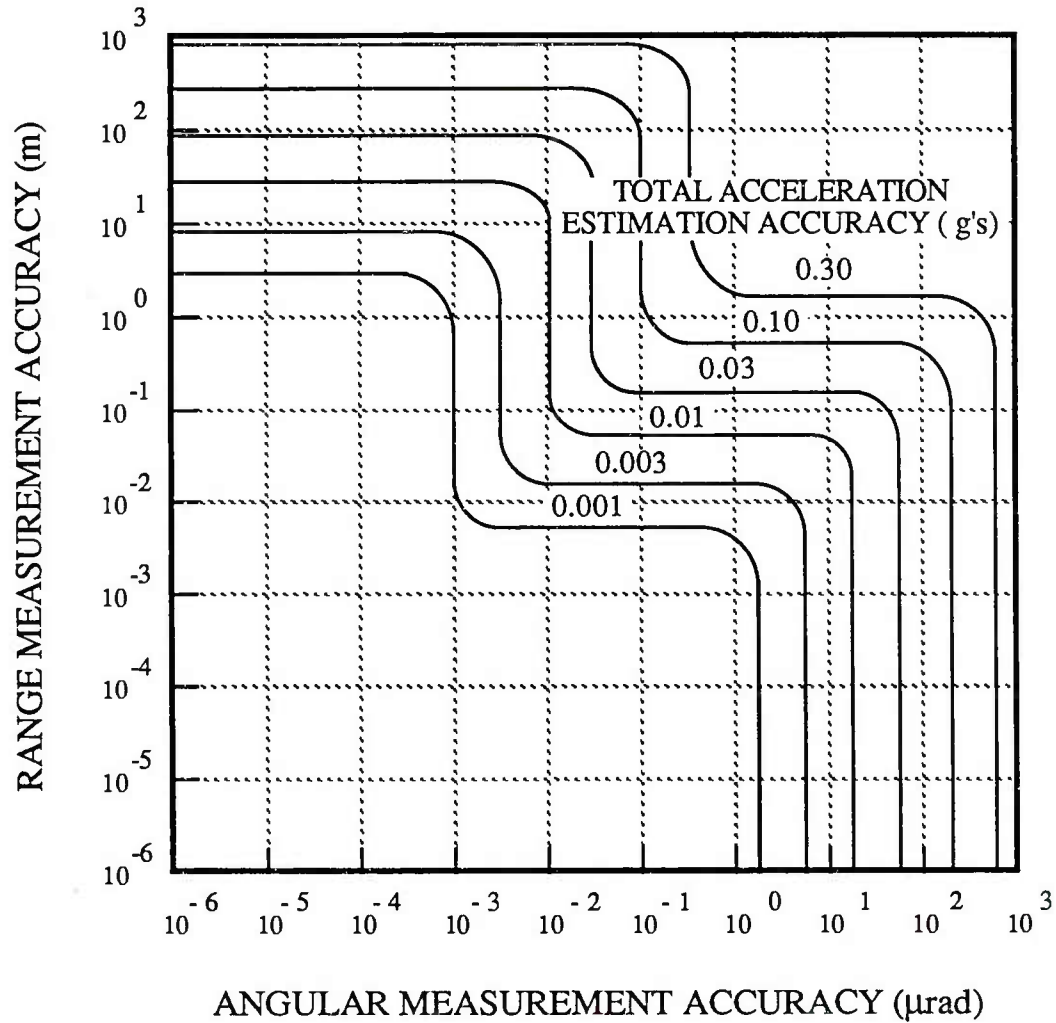
17

Figure 10. Contours of constant overall acceleration estimation accuracy as a function of radar angle and range measurement accuracies with $\sigma_\alpha = 0°$.

18

R = 3000 km   V = 7 km/sec.   a = 0.2 g

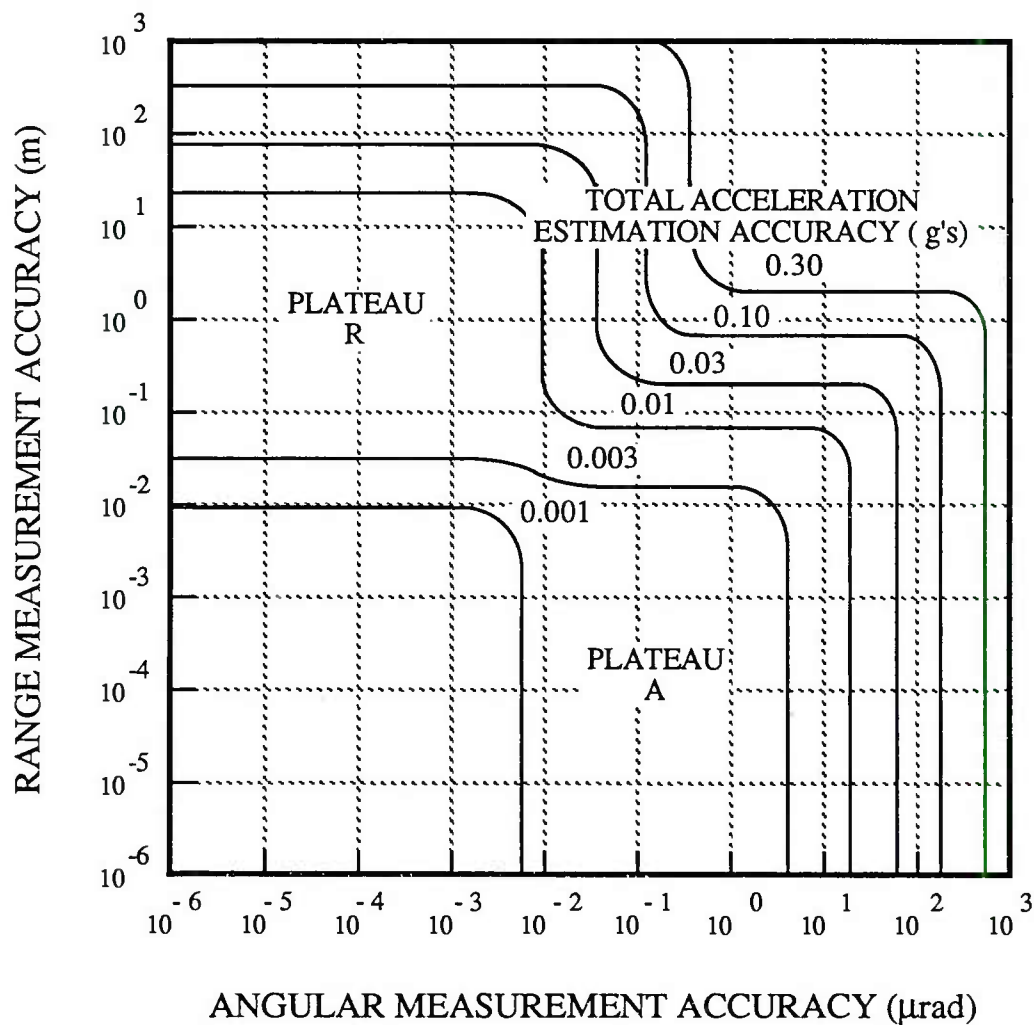α = 30°   ß = 60°   PRF = 10 Hz.   NT = 2 sec

Figure 11. Contours of constant overall acceleration estimation accuracy as a function of radar angle and range measurement accuracies with $\sigma_\alpha = 1°$.

19

R = 3000 km   V = 7 km/sec.   a = 0.2 g

α = 30°   ß = 60°   PRF = 10 Hz.   NT = 2 sec

Figure 12. Contours of constant overall acceleration estimation accuracy as a function of radar angle and range measurement accuracies with $\sigma_\alpha = 10°$.

R = 3000 km   V = 7 km/sec.   a = 0.2 g

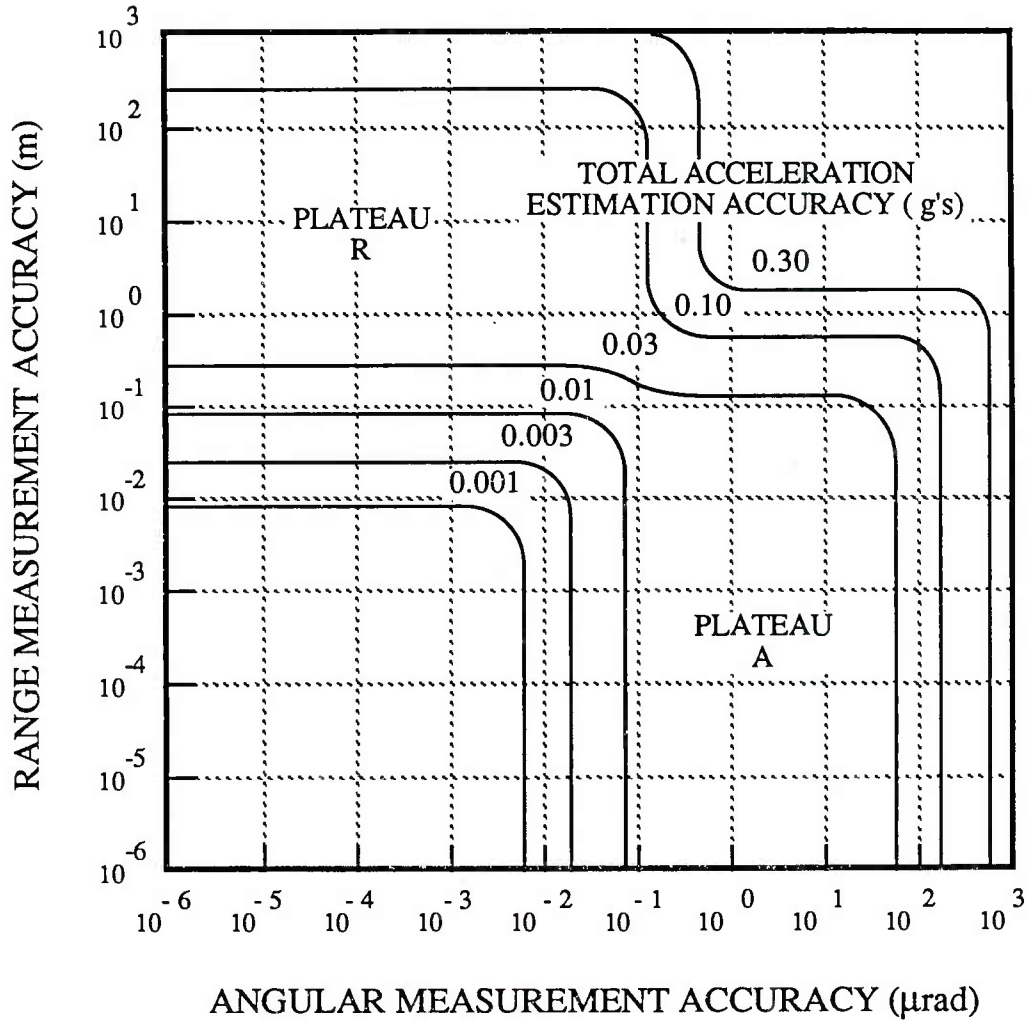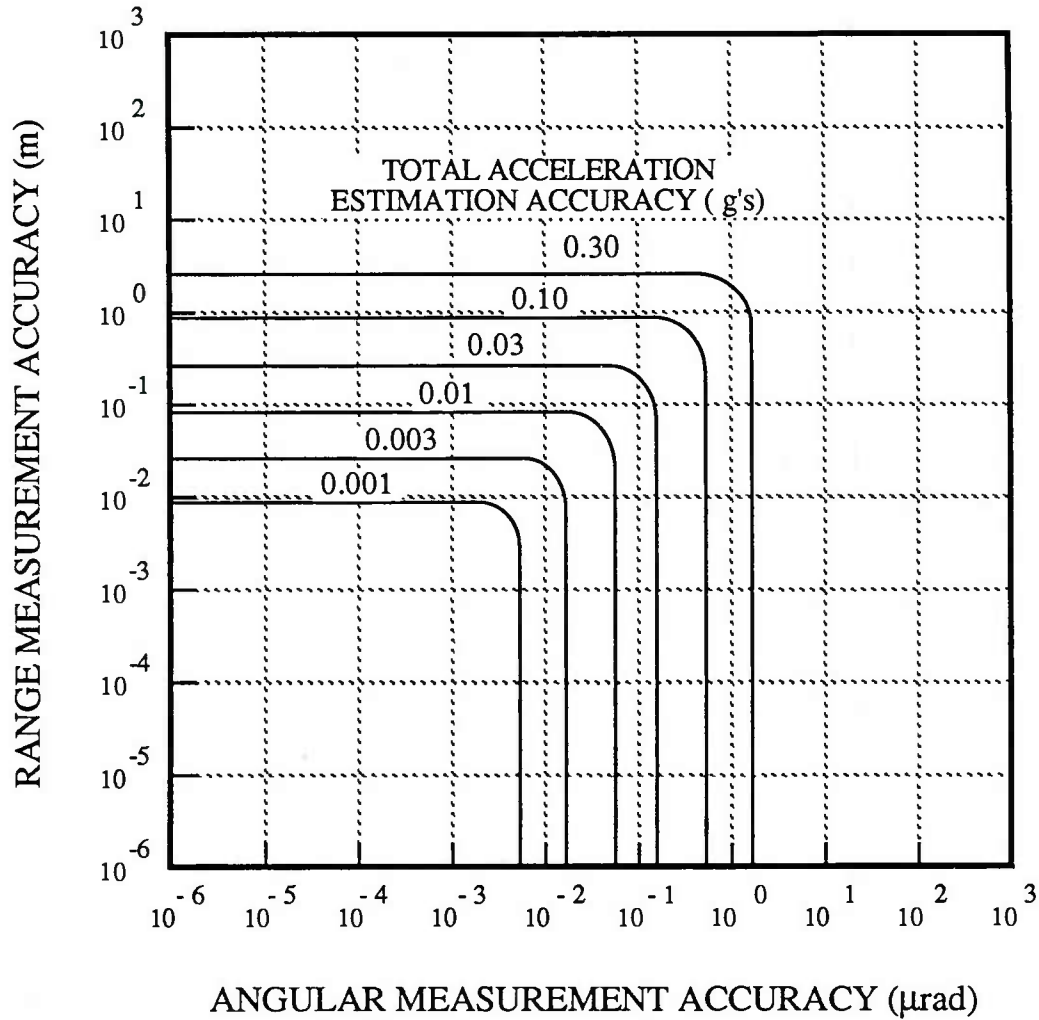α = 30°   ß = 60°   PRF = 10 Hz.   NT = 2 sec

Figure 13. Contours of constant overall acceleration estimation accuracy as a function of radar angle and range measurement accuracies with $\sigma_\alpha = \infty°$.

21

R = 3000 km V = 7 km/sec. a = 0.2 g

α = 30° ß = 60° PRF = 10 Hz. NT = 2 sec

Figure 14. 3-D graph of overall acceleration estimation accuracy as a function of radar angle and range measurement accuracies with $\sigma_\alpha = 0°$.

R = 3000 km   V = 7 km/sec.   a = 0.2 g

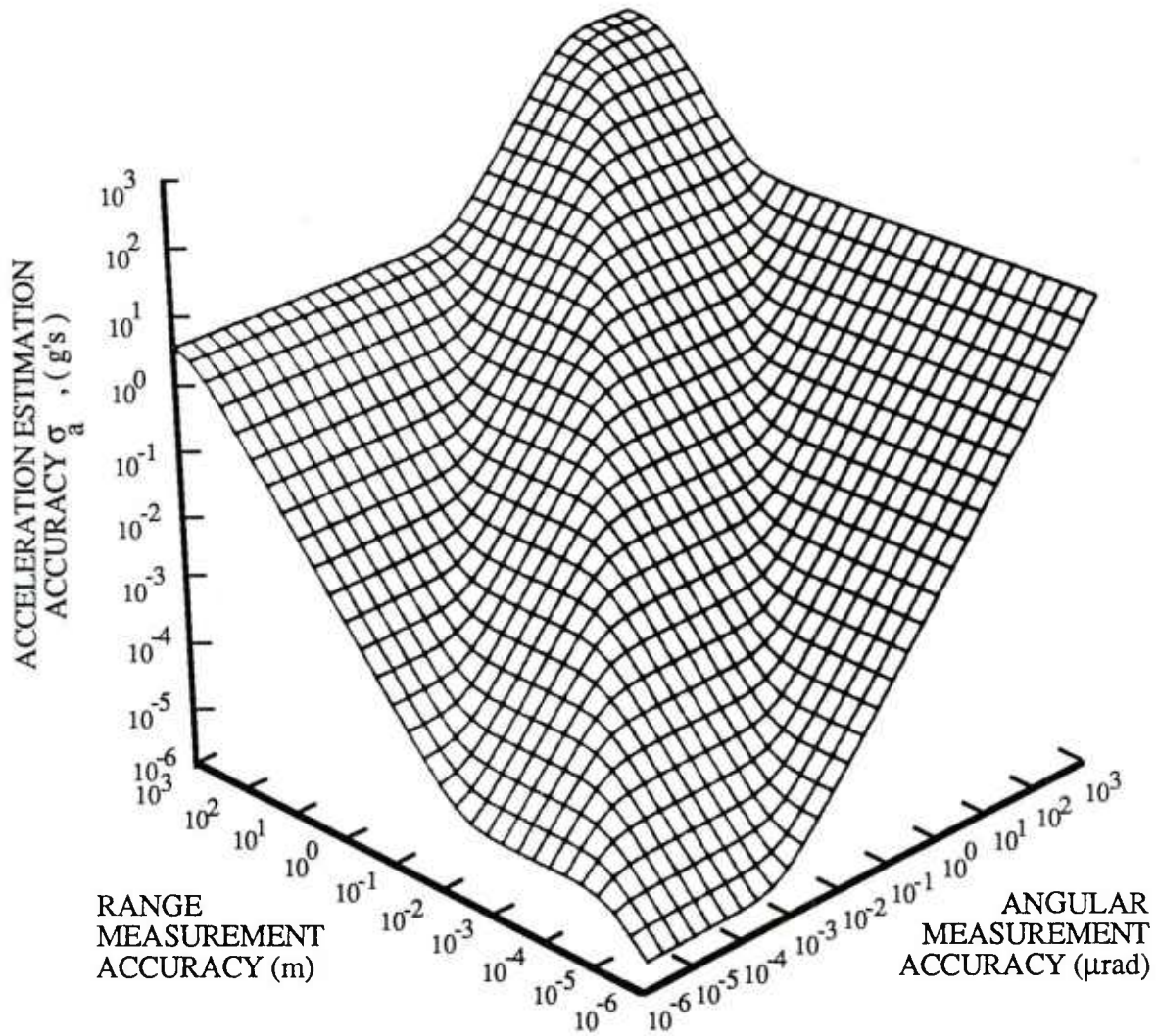α = 30°   ß = 60°   PRF = 10 Hz.   NT = 2 sec

Figure 15.   3-D graph of overall acceleration estimation accuracy as a function of radar angle and range measurement accuracies with $\sigma_\alpha = 1°$.

$R = 3000$ km $V = 7$ km/sec. $a = 0.2$ g

$\alpha = 30°$ $ß = 60°$ $PRF = 10$ Hz. $NT = 2$ sec
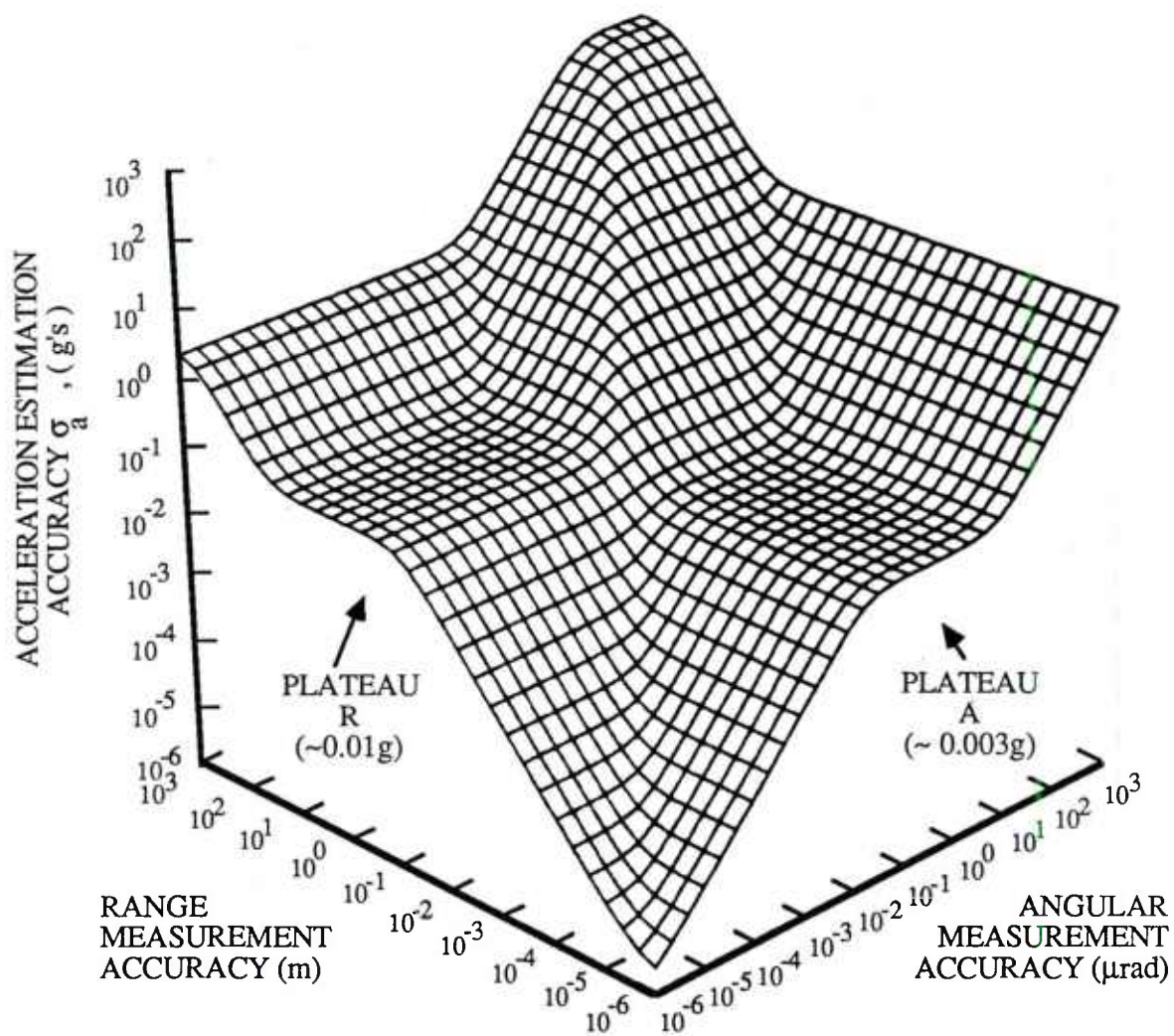

Figure 16. 3-D graph of overall acceleration estimation accuracy as a function of radar angle and range measurement accuracies with $\sigma_{\alpha} = 10°$.

$$R = 3000 \text{ km} \qquad V = 7 \text{ km/sec.} \qquad a = 0.2 \text{ g}$$

$$\alpha = 30° \qquad \beta = 60° \qquad PRF = 10 \text{ Hz.} \qquad NT = 2 \text{ sec}$$

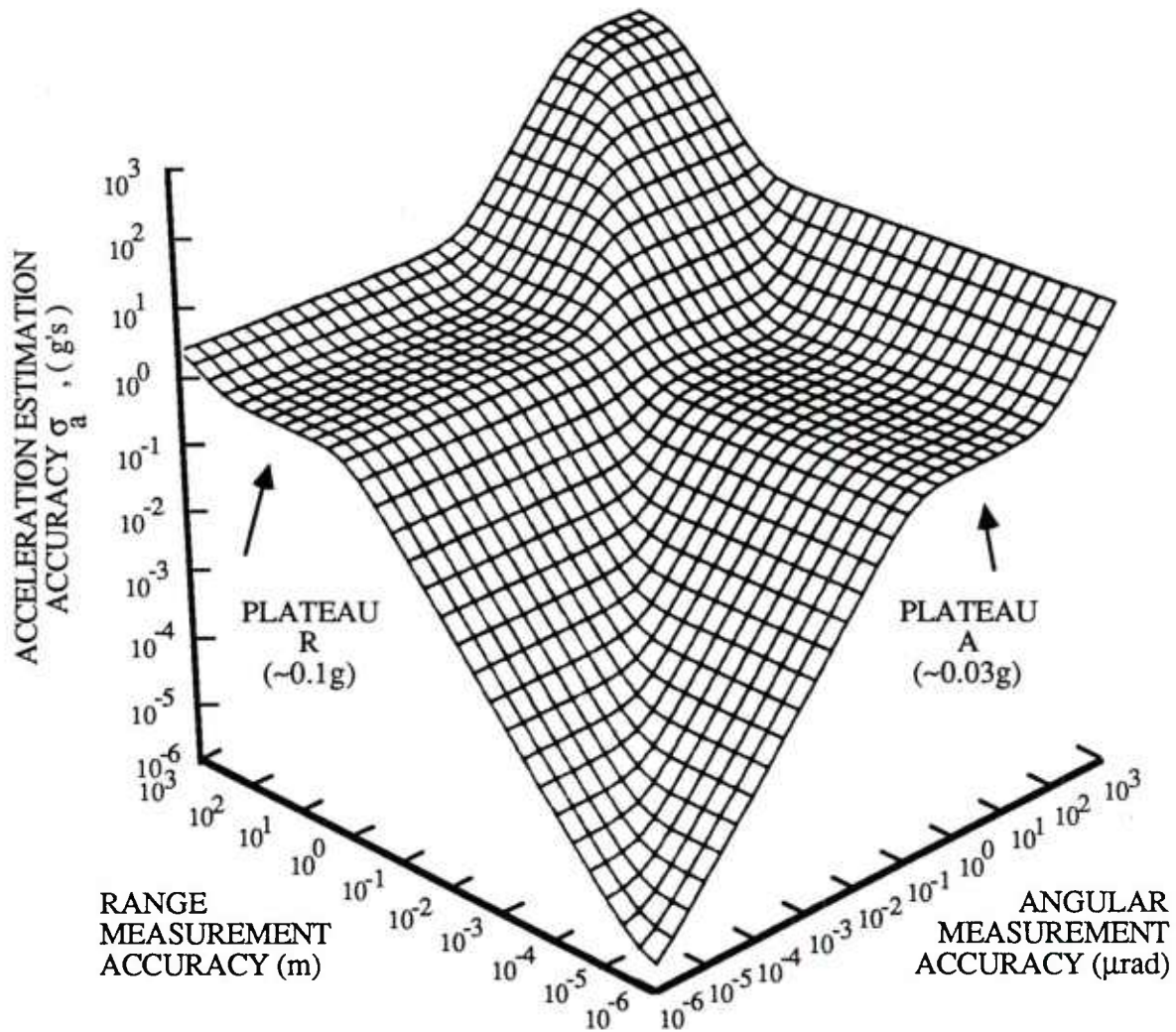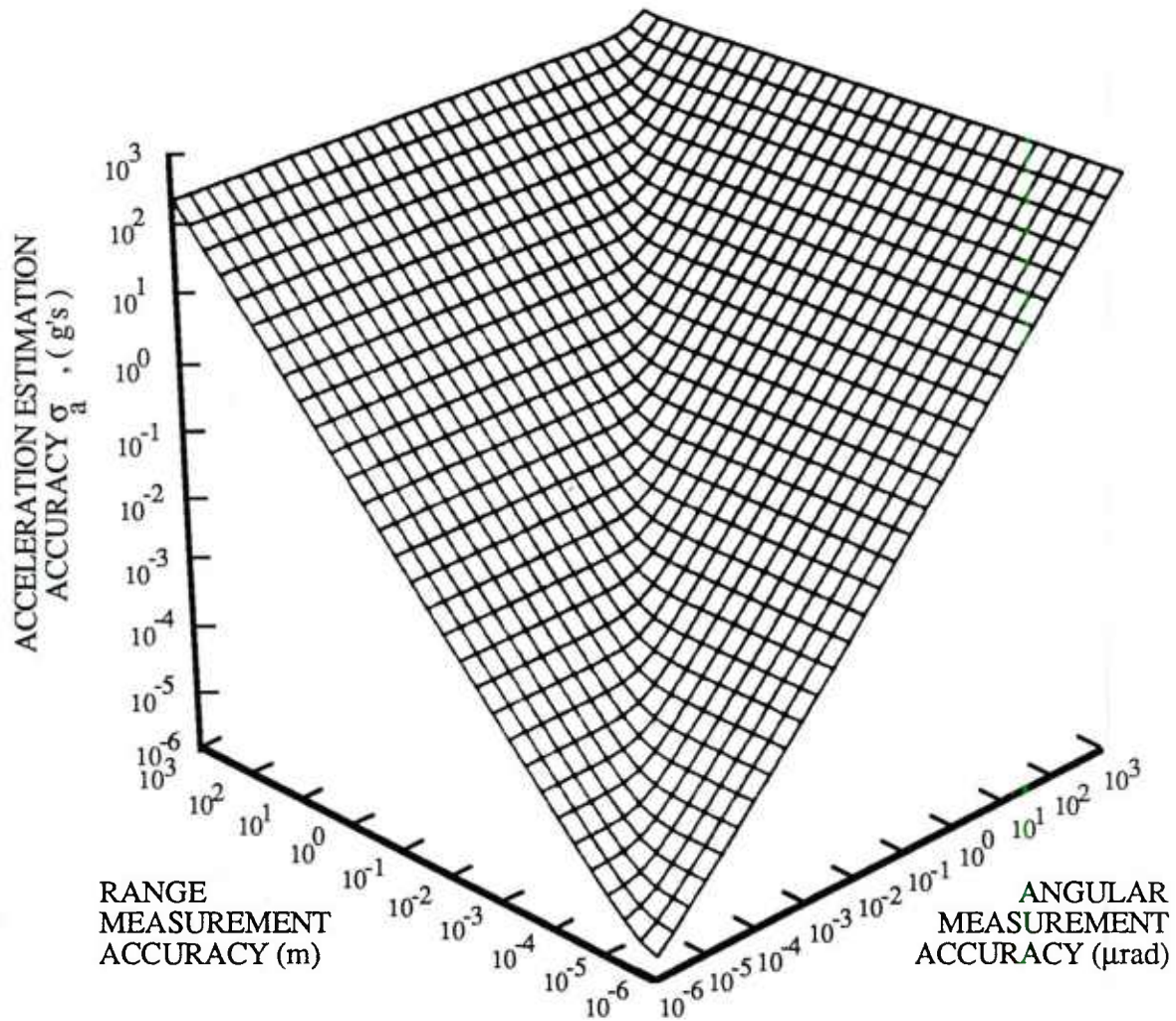
Figure 17. 3-D graph of overall acceleration estimation accuracy as a function of radar angle and range measurement accuracies with $\sigma_\alpha = \infty°$.

25
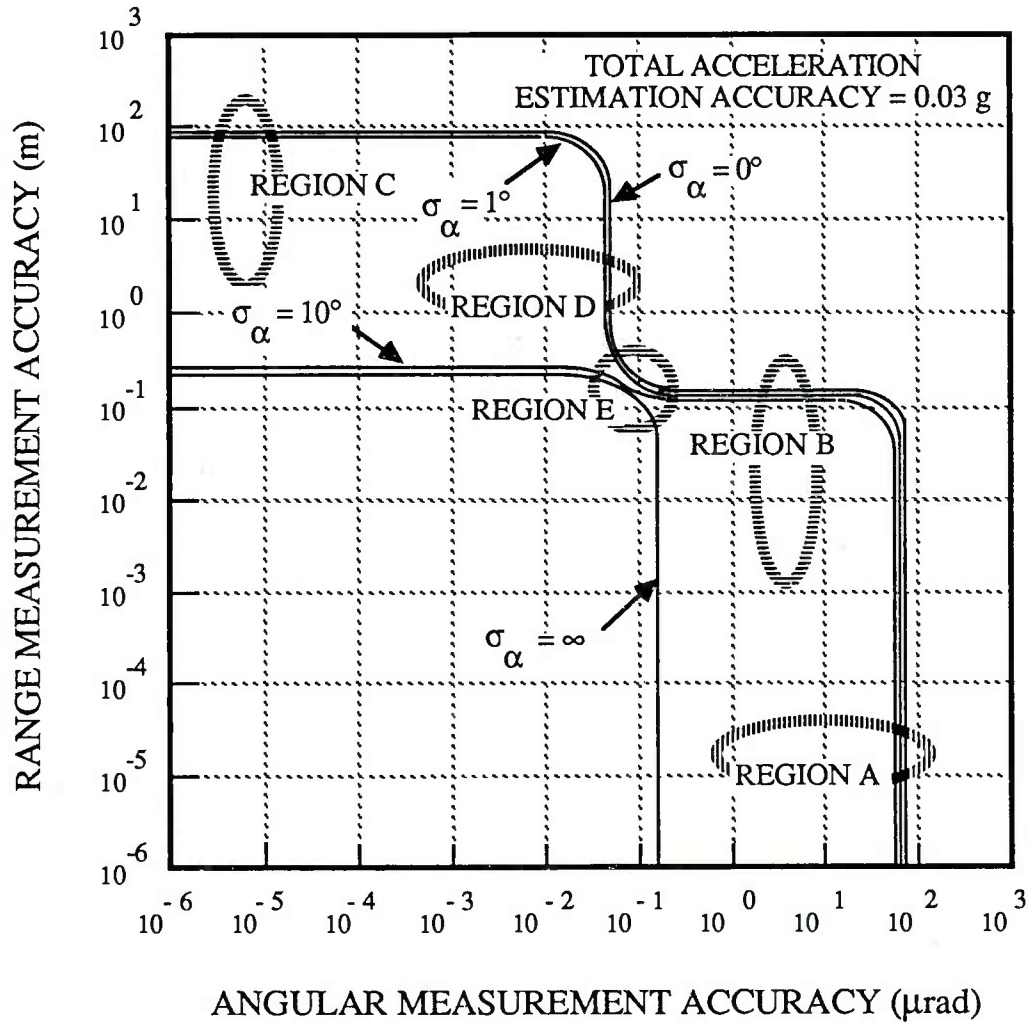
Figure 18. Contours of overall acceleration estimation accuracy of 0.03g as a function of radar angle and range measurement accuracies and various σ_α values.

R = 3000 km   V = 7 km/sec.   a = 0.2 g

α = 30°   ß = 60°   NT = 10 sec ϵ_R = 0.003 m

Figure 19. Overall acceleration estimation accuracy as a function of PRF and angular measurement accuracy for a fixed range measurement accuracy and total track time with $\sigma_\alpha = 0°$.

27

Figure 20. Overall acceleration estimation accuracy as a function of total track time and angular measurement accuracy for a fixed range measurement accuracy and PRF with $\sigma_{\alpha} = 0°$.

28

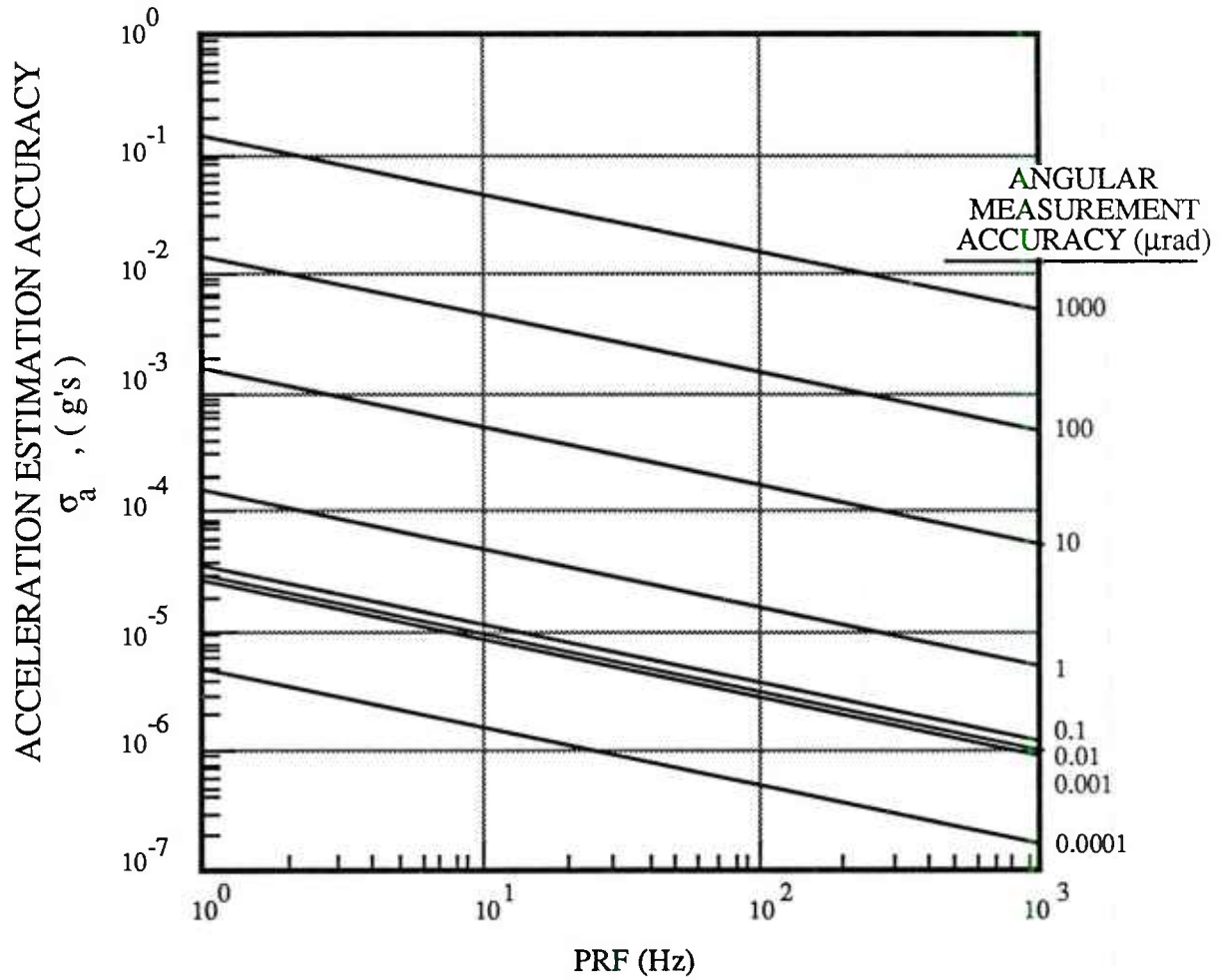Figure 21. Overall acceleration estimation accuracy as a function of PRF and angular measurement accuracy for a fixed range measurement accuracy and total track time with $\sigma_\alpha = \infty$.

29

R = 3000 km   V = 7 km/sec.   a = 0.2 g

α = 30°   ß = 60°   PRF = 10 Hz. ε_R = 0.003 m
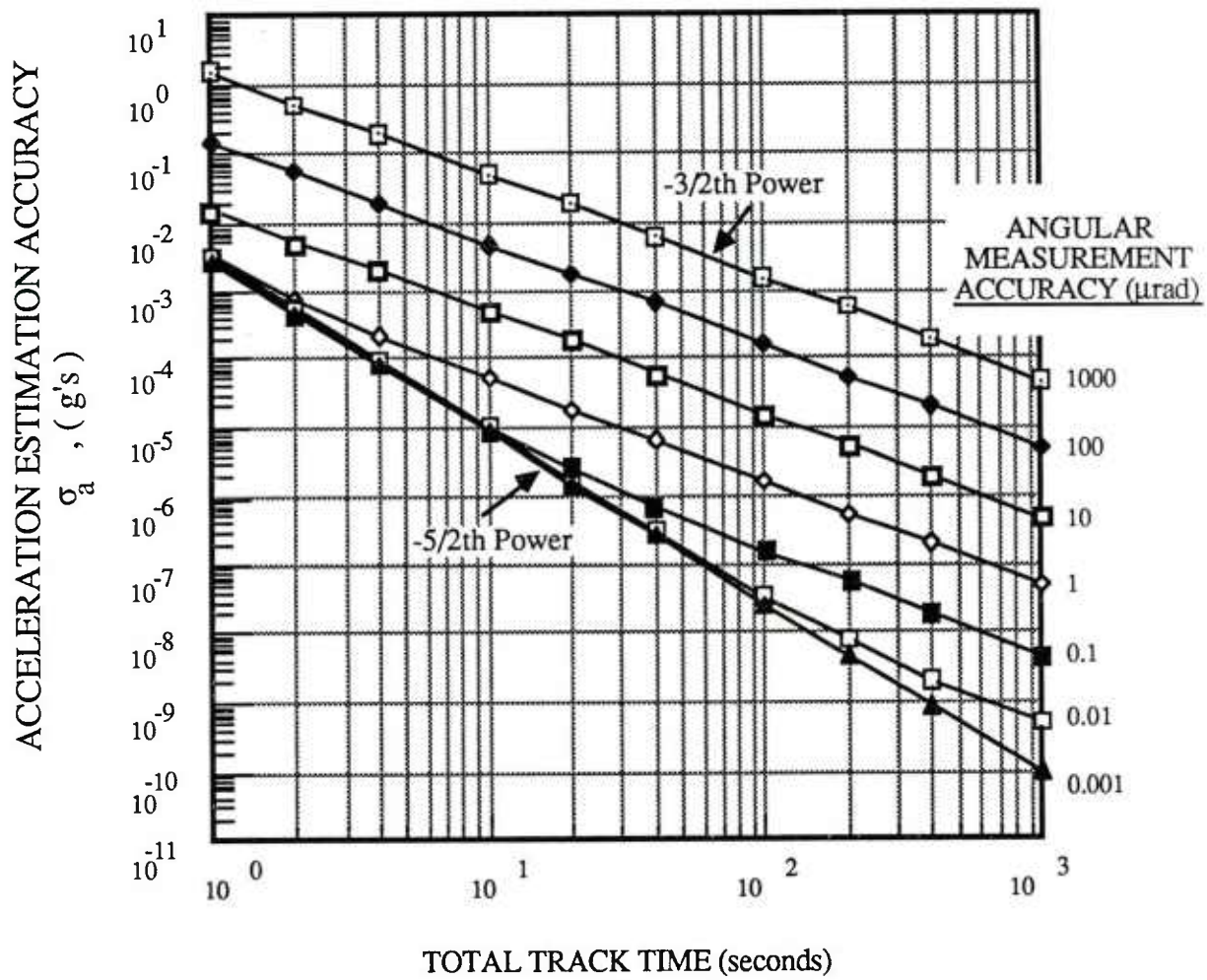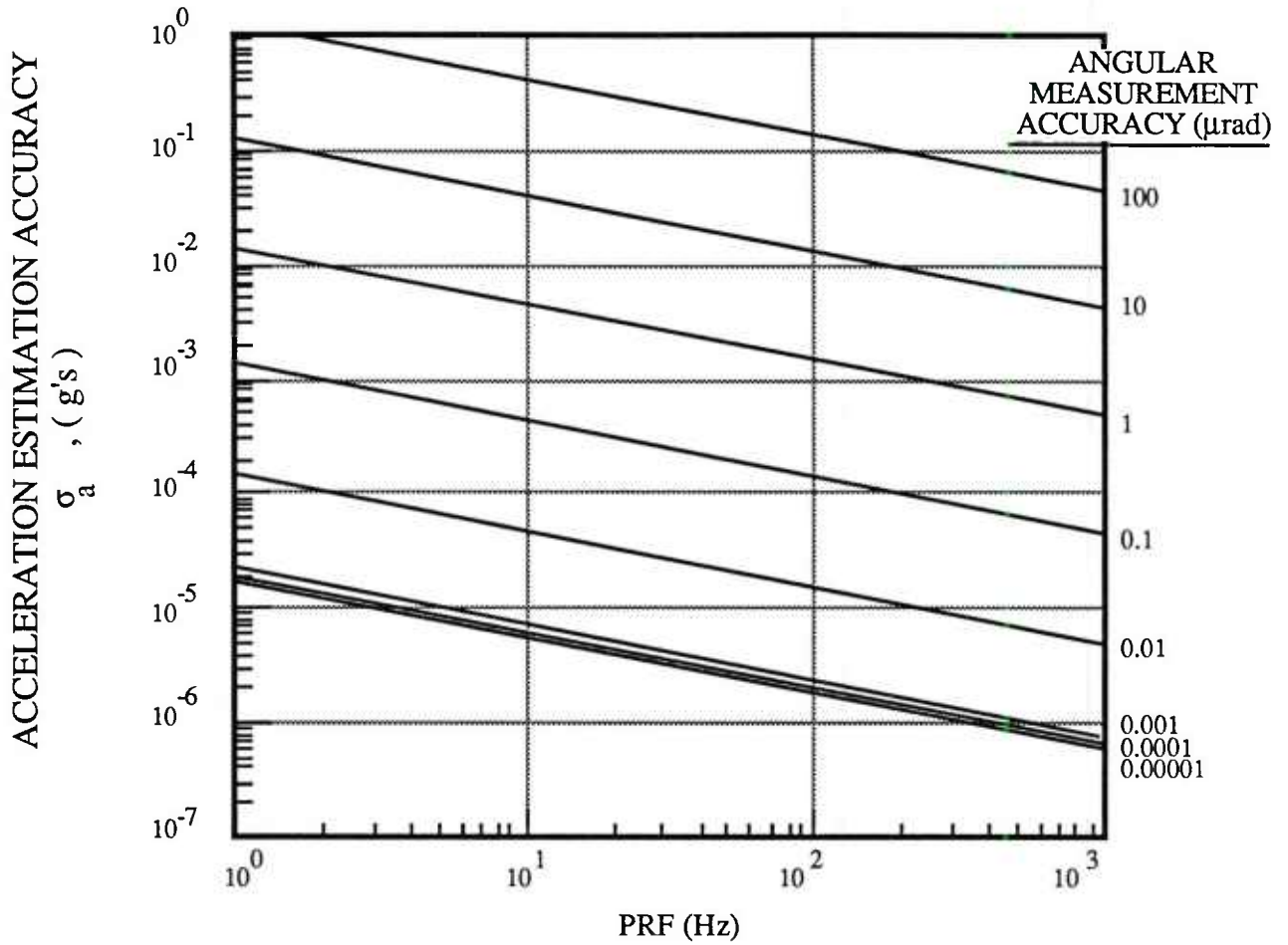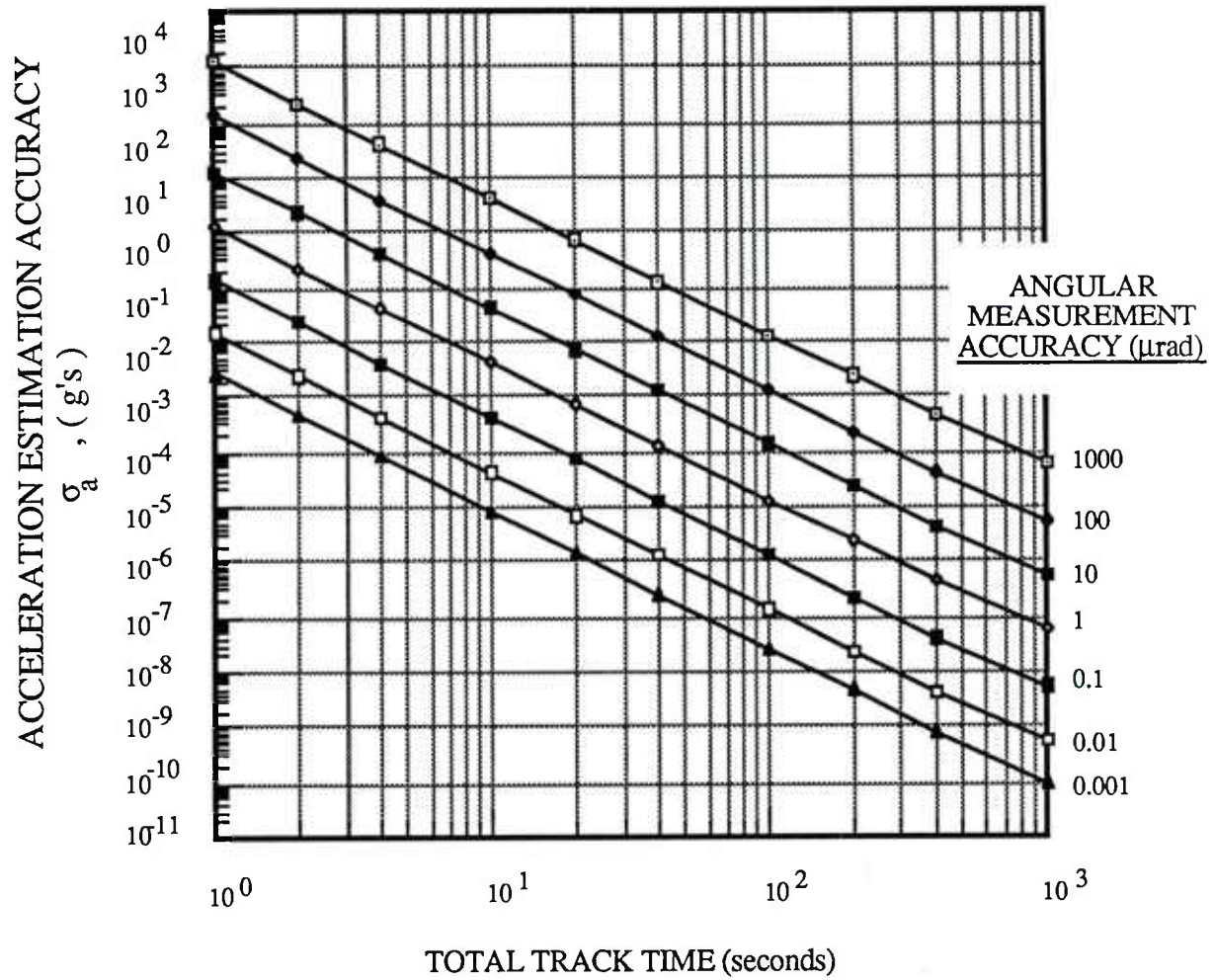
Figure 22. Overall acceleration estimation accuracy as a function of total track time and angular measurement accuracy for a fixed range measurement accuracy and PRF with $\sigma_\alpha = \infty$

30
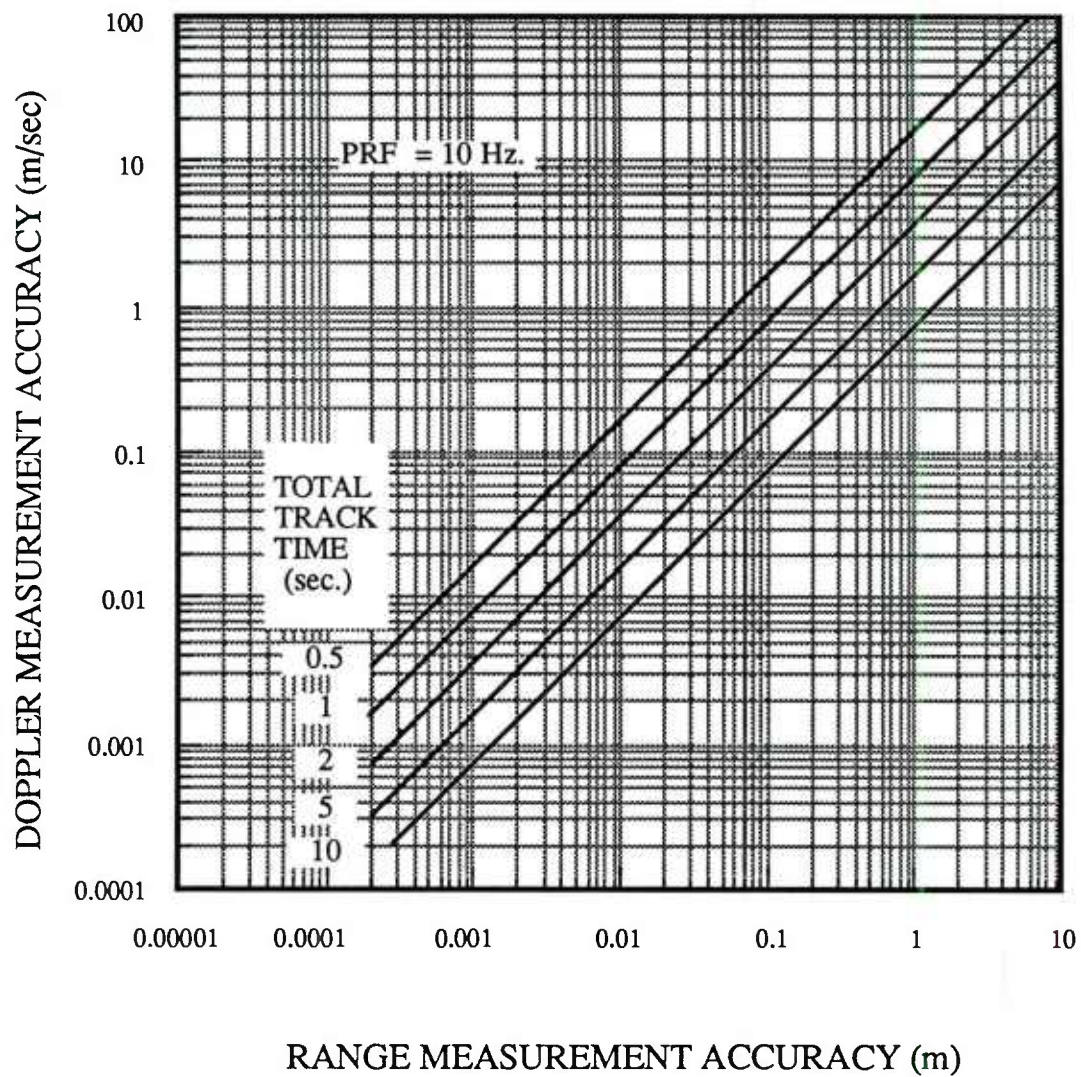
Figure 23. Equivalent radar range and Doppler measurement accuracies for a given PRF and total track time.

IV. SUMMARY

An analytical formula for calculating lower bounds on acceleration measurement accuracy with given sensor-target geometry, sensor range (or Doppler) and angle measurement accuracies, data rate (PRF) and total track time is presented. Numerical examples and interpretations of these results are also given. Some scaling rules and simple approximations are presented for quick calculations to obtain an idea of the trade-offs between several radar parameters.

To summarize these major results:

1. The accuracy of acceleration components in both range and angle are functions of the sensor range (or Doppler) and angle accuracy. These component accuracies have asymptotes proportional to the range or cross-range accuracy. Each component accuracy scales with $(PRF)^{-1/2}$ and $(track\ time)^{-3/2}$ or $(track\ time)^{-5/2}$.

2. The overall acceleration accuracy is limited by the more accurate component if the direction of the acceleration is known and by the less accurate component if the direction is not known.

3. The combination of range and angle errors with errors in direction result in significant "thresholds" and "plateaus" in performance as a function of radar parameters.

APPENDIX

VELOCITY AND ACCELERATION ESTIMATION ACCURACY OBTAINED BY POLYNOMIAL SMOOTHING

Consider a sensor which measures range, angle and Doppler on a target with single hit accuracy ε_R, ε_θ, and $\varepsilon_{\dot{R}}$, respectively. N samples with sampling period T are obtained from a target; the velocity and acceleration estimation accuracies at the center of data interval after polynomial smoothing are [3]:

$$\sigma_{\dot{R}}^2 = \left[\left[\frac{\varepsilon_{\dot{R}}^2}{N} \right]^{-1} + \left[\frac{12\varepsilon_R^2}{N(N^2-1)T^2} \right]^{-1} \right]^{-1} \tag{A.1}$$

$$\sigma_{\ddot{R}}^2 = \left[\left[\frac{12\varepsilon_{\dot{R}}^2}{N(N^2-1)T^2} \right]^{-1} + \left[\frac{720\varepsilon_R^2}{N(N^2-1)(N^2-4)T^4} \right]^{-1} \right]^{-1} \tag{A.2}$$

$$\sigma_{\dot{\theta}}^2 = \frac{12\varepsilon_\theta^2}{N(N^2-1)T^2} \tag{A.3}$$

$$\sigma_{\ddot{\theta}}^2 = \frac{720\varepsilon_\theta^2}{N(N^2-1)(N^2-4)T^4} \tag{A.4}$$

33

ACKNOWLEDGEMENT

REFERENCES

[1] C. B. Chang, "Ballistic Trajectory Estimation with Angle-Only Measurements," IEEE Trans. Automat. Contr. AC-25, 474 (1980).

[2] H. L. Van Trees, Detection, Estimation and Modulation Theory, Part I (Wiley, New York, 1968).

[3] R.W. Miller and C.B. Chang, private communication.

REPORT DOCUMENTATION PAGE

1a. REPORT SECURITY CLASSIFICATION Unclassified	1b. RESTRICTIVE MARKINGS
2a. SECURITY CLASSIFICATION AUTHORITY	3. DISTRIBUTION/AVAILABILITY OF REPORT Approved for public release; distribution unlimited.
2b. DECLASSIFICATION/DOWNGRADING SCHEDULE	

4. PERFORMING ORGANIZATION REPORT NUMBER(S) Technical Report 790	5. MONITORING ORGANIZATION REPORT NUMBER(S) ESD-TR-87-080

6a. NAME OF PERFORMING ORGANIZATION Lincoln Laboratory, MIT	6b. OFFICE SYMBOL (If applicable)	7a. NAME OF MONITORING ORGANIZATION Electronic Systems Division
6c. ADDRESS (City, State, and Zip Code) P.O. Box 73 Lexington, MA 02173-0073		7b. ADDRESS (City, State, and Zip Code) Hanscom AFB, MA 01731

8a. NAME OF FUNDING/SPONSORING ORGANIZATION Department of the Navy for SDIO	8b. OFFICE SYMBOL (If applicable)	9. PROCUREMENT INSTRUMENT IDENTIFICATION NUMBER F19628-85-C-0002

8c. ADDRESS (City, State, and Zip Code)
Space and Naval Warfare Systems Command
Strategic Defense Systems Program Office
PMW-145
Crystal Mall No. 2, Washington, DC 20362

10. SOURCE OF FUNDING NUMBERS

PROGRAM ELEMENT NO.	PROJECT NO.	TASK NO.	WORK UNIT ACCESSION NO.
63220C			

11. TITLE (Include Security Classification)

Lower Bounds on Acceleration Estimation Accuracy

12. PERSONAL AUTHOR(S)
Keh-Ping Dunn

13a. TYPE OF REPORT Technical Report	13b. TIME COVERED FROM _____ TO _____	14. DATE OF REPORT (Year, Month, Day) 1987, October, 5	15. PAGE COUNT 44

16. SUPPLEMENTARY NOTATION

None

17.	COSATI CODES		18. SUBJECT TERMS (Continue on reverse if necessary and identify by block number)
FIELD	GROUP	SUB-GROUP	acceleration measurement lower bounds
			sensor-target geometry sensor trade-off
			sensor parameters

19. ABSTRACT (Continue on reverse if necessary and identify by block number)

Estimation lower bounds on the accuracy of radar measurement of the acceleration of a moving target are derived. These bounds are expressed in terms of the sensor parameters, such as: range (or Doppler) and angle accuracies, track time, data rate (PRF), and an *a priori* estimate of the direction of the target acceleration. Simple scaling laws that allow the reader to trade-off these parameters utilizing curves presented in this report are also given.

20. DISTRIBUTION/AVAILABILITY OF ABSTRACT ☐ UNCLASSIFIED/UNLIMITED ☒ SAME AS RPT. ☐ DTIC USERS	21. ABSTRACT SECURITY CLASSIFICATION Unclassified
22a. NAME OF RESPONSIBLE INDIVIDUAL Capt. Arthur H. Wendel, USAF	22b. TELEPHONE (Include Area Code) (617) 863-5500, Ext. 2330 22c. OFFICE SYMBOL ESD/TML